Anophelin: Kinetics and Mechanism of Thrombin Inhibition

Ivo M. B. Francischetti, Jesus G. Valenzuela, and José M. C. Ribeiro*

Medical Entomology Section, Laboratory of Parasitic Diseases, National Institute of Allergy and Infectious Diseases, National Institutes of Health, Bethesda, Maryland 20892-0425

Received June 1, 1999; Revised Manuscript Received September 16, 1999

ABSTRACT: Anophelin is a 6.5-kDa peptide isolated from the salivary gland of *Anopheles albimanus* that behaves as an α-thrombin inhibitor. In this paper, kinetic analyses and the study of mechanism of α-thrombin inhibition by anophelin were performed. Anophelin was determined to be a reversible, slow, tight-binding inhibitor of α-thrombin, displaying a competitive type of inhibition. The binding of anophelin to α-thrombin is stoichiometric with a dissociation constant (K_i) of 5.87 ± 1.46 pM, a calculated association rate constant (k_1) of 2.11 ± 0.06 × 10^8 M^{-1} s^{-1}, and a dissociation rate constant (k_{-1}) of 4.05 ± 0.97 × 10^{-4} s^{-1}. In the presence of 0.15 and 0.4 M NaCl, a 17.6- and 207-fold increase in the K_i of anophelin−α-thrombin complex was observed, respectively, indicating that ionic interactions are important in anophelin−α-thrombin complex formation. Incubation of α-thrombin with C-terminal hirudin fragment 54−65 that binds to α-thrombin anion binding exosite 1 (TABE1) attenuates α-thrombin inhibition by anophelin; anophelin also blocks TABE1-dependent trypsin-mediated proteolysis of α-thrombin. Using γ-thrombin, an α-thrombin derivative where the anion binding exosite has been disrupted, anophelin behaves as a fast and classical competitive inhibitor of γ-thrombin hydrolysis of small chromogenic substrate (K_i = 0.694 ± 0.063 nM). In addition, anophelin−γ-thrombin complex formation is prevented by treatment of the enzyme with D-Phe-Pro-Arg-chloromethyl ketone (PPACK), a reagent that irreversibly blocks the catalytic site of thrombin. It is concluded that anophelin is a potent dual inhibitor of α-thrombin because it binds both to TABE1 and to the catalytic site, optimal binding being dependent on the availability of both domains. Finally, anophelin inhibits clot-bound α-thrombin with an IC_{50} of 45 nM and increases the lag phase that precedes explosive in vitro α-thrombin generation after activation of intrinsic pathway of blood coagulation. Because of its unique primary sequence, anophelin may be used as a novel reagent to study the structure and function of α-thrombin.

α-Thrombin (EC 3.4.21.5) plays a central role in blood coagulation. Its primary function is to cleave fibrinogen generating fibrin and an insoluble clot. In addition, it has regulatory functions in the activation of blood coagulation factors V, VIII, XI, and XIII and protein C in the coagulation cascade (*1*). α-Thrombin also activates a number of cells, including endothelial cells and platelets. The diverse biological functions of α-thrombin rely on its complex tertiary structure comprising different domains specialized in specific thrombin interactions. In fact, the crystal structure of human α-thrombin reveals that prominent structural features of the α-thrombin molecule are a catalytic triad within a deep canyon-like active site cleft and two extended surfaces that are mainly composed of positively charged residues known as exosite 1 (TABE1)[1] and exosite 2 (TABE2) (*2*−*4*). Exosite 1 is required for α-thrombin binding to fibrinogen (*5*), heparin cofactor II (*6*), thrombomodulin (*7*, *8*), and GPIb (*9*−*12*). Exosite 2, which is located close to the carboxy-terminal B-chain helix, is involved in heparin-modulated inhibition by the serpins antithrombin and proteinase nexin I (*13*, *14*).

The pivotal role of α-thrombin in the physiologic blood coagulation cascade as well as in thrombotic events indicates that α-thrombin may be the target of inhibitors that could regulate the function of the enzyme. In addition, evolutionary pressure has selected a number of biologically active substances from blood-sucking animals in order to inhibit thrombin. Actually, α-thrombin inhibitors have been isolated from such distinct sources as insects (*15*), leeches (*16*), snake venoms (*17*), and plants (*18*). The mechanism of α-thrombin inhibition by such molecules has been the focus of several studies. While some of these inhibitors block thrombin's catalytic site, others are exclusive ligands of the α-thrombin anion binding exosite(s), and still others are dual inhibitors, binding to both domains (*19*−*21*).

Our aim in this study has been to extend the characterization of the mechanism of α-thrombin inhibition by anophelin, a 6.5-kDa peptide isolated from *Anopheles albimanus* (*22*). Anophelin's K_i is in the low picomolar range, and it forms an equimolecular complex of high affinity with α-thrombin but does not interact with prothrombin, factor X, or factor Xa. In this paper, we provide experimental evidence suggesting that anophelin binds both to the catalytic site and to TABE1 of α-thrombin.

* To whom correspondence should be addressed: Medical Entomology Section, LPD, NIAID, Bldg 4, Rm 126, 4 Center Dr., Bethesda, MD 20892-0425. Phone: 301-402-2748. Fax: 301-402-4941. E-mail: jribeiro@nih.gov.

[1] Abbreviations: APTT, activated partial thromboplastin time; K_i, inhibition constant; K_i*, apparent inhibition constant; K_m, Michaelis−Menten constant; K_{obs}, apparent first-order rate constant; PPACK, D-Phe-Pro-Arg-chloromethyl ketone; TABE, α-thrombin anion binding exosite.

10.1021/bi991231p
Published on Web 11/23/1999

MATERIALS AND METHODS

Materials. Anophelin was synthesized as described (*22*). α-Thrombin, prothrombin, factor X, factor Xa, and D-Phe-Pro-Arg-chloromethyl ketone (PPACK) were purchased from CalBiochem (San Diego, CA). Chromogenic substrate for trypsin (Chromozym X, Chromogenix) was obtained from Boehringer Mannheim (Indianapolis, IN). S-2238 (H-D-phenylalanyl-L-pipecolyl-L-arginine-*p*-nitroaniline dihydrochloride) was obtained from Chromogenix (Milano, Italy). γ-Thrombin was purchased from Enzyme Research Laboratories (South Bend, IN). Activated partial thromboplastin time (APTT) reagent, fibrinogen, trypsin, hirudin, and [Tyr-$(SO_3H)^{63}$]-hirudin fragment 54−65 were purchased from Sigma Chemical Co. (St. Louis, MO). BCA protein reagents A and B were purchased from Pierce (Rockford, IL). Other reagents were of analytical grade and obtained from Merck Research Laboratories (Darmstadt, Germany) or Sigma Chemical Co. (St. Louis, MO).

Chromogenic Substrate Hydrolysis by α-Thrombin and γ-Thrombin. Chromogenic substrate hydrolysis was detected using a Thermomax microplate ELISA reader (Molecular Devices, Sunnyvale, CA) equipped with an microplate mixer and heating system in addition to a kinetic module software and processed as described (*22*). Chromogenic substrate hydrolysis was followed by reading at 405 nm, at 37 °C. In the several kinetic assays, anophelin was incubated with chromogenic substrate followed by addition of α- or γ-thrombin, as indicated in the figure legends. Alternatively, reactions were started by addition of chromogenic substrate to a mixture containing anophelin and α- or γ-thrombin. In all kinetic measurements care was taken to ensure that substrate was less than 20% hydrolyzed. The total volume of the reaction was 200 μL. In some experiments, C-terminal hirudin fragment 54−65 was incubated with α-thrombin for 20 min at 37 °C, followed by addition of anophelin. All reagents were diluted in the reaction buffer, Hepes−BSA (50 mM Hepes, 0.5% BSA, pH 7.4). Studies of the effects of anophelin on trypsin proteolytic activity were performed in the same buffer except that 630 μM Chromozym X was used to start reactions. To irreversibly block the catalytic sites of the enzymes, α-thrombin (0.83 μM) and γ-thrombin (0.8 μM) were incubated with PPACK (5 μM) in 0.75 M NaCl, 100 mM Tris, pH 8.0, for 30 min at room temperature, followed by several washings (with Hepes 50 mM, pH 7.4) and concentration of the samples in 3-kDa cutoff Microcon (Millipore Co., Bedford), at 4 °C. The K_m of α-thrombin for S-2238 was 8.3 ± 0.6 and 6.7 ± 0.43 μM at 0 and 0.15 M NaCl, respectively. For γ-thrombin, the K_m for S-2238 was 28.8 ± 0.87 μM at 0 M NaCl. Data points were fit by nonlinear regression according to the best sum of squares dictated by equations described in the text.

Nondenaturing Gel Electrophoresis. To detect complex formation, anophelin (4.5 μM, final concentration) was preincubated for 30 min with increasing concentrations of α-thrombin (1.38−8.3 μM, final concentrations) in 50 mM Hepes, pH 7.4, forming a total volume of 30 μL. Aliquots (0.5 μL) of α-thrombin were taken before and after addition of anophelin and diluted in 1000 μL of 50 mM Hepes, BSA 0.5%, pH 7.4. Then, 90 μL of this sample was taken to detect residual α-thrombin activity, by addition of 10 μL of S-2238 (500 μM, final concentration). Reactions were followed for 10 min, and α-thrombin inhibition was estimated according to a decrease in the initial velocity of α-thrombin activity. The remaining sample (29.0 μL) was applied to 4−20% SDS−PAGE using a NOVEX Powereasy500 apparatus; the migration buffer consisted of 68.5 mM Tris at pH 8.8. Proteins were stained with Coomassie Brilliant Blue G and destained in 15% methanol, 10% acetic acid. Gels were scanned (Hewlett-Packard Scanjet 4p), and densitometry of bands was performed to quantify complex formation. In some experiments, anophelin (10 μM) was incubated with γ-thrombin (4 μM) or PPACK-γ-thrombin (4 μM), prothrombin (6.9 μM), factor X (6.9 μM), and factor Xa (6.9 μM), in Hepes 50 mM, pH 7.4, forming a total volume of 30 μL. Complex formation was analyzed by 4−20% PAGE under nondenaturing conditions, as described above. Inhibition of trypsin-mediated α-thrombin proteolysis by anophelin was performed by incubation of α-thrombin (4.1 μM, 47 pmol) with buffer or anophelin (10 μM) for 10 min in the absence or presence of 250 ng of trypsin, in Hepes 50 mM, pH 7.4, forming a total volume of 10 μL. Mixtures were incubated for 1 h at 37 °C, and reactions were terminated by addition of Laemmli buffer containing SDS 2% and β-mercaptoethanol 5% (final concentrations) and boiling for 5 min. Formation of complex was performed by 4−20% SDS−PAGE, as described above.

Clot-Bound α-Thrombin. Clot-bound α-thrombin was tested for its activity on chromogenic substrate hydrolysis. Fibrin clots were prepared by incubating 300 μL of purified fibrinogen (2 mg/mL in 50 mM Hepes, pH 7.5, 150 mM NaCl, 10 mg/mL $CaCl_2$) with 30 nM α-thrombin. After 2 h at 37 °C, the clots were extensively washed in the same buffer, which was changed eight times over a period of 24 h. The clots were then carefully transferred to a new Eppendorf tube and incubated with 200 μL of increasing concentrations of anophelin (diluted in 50 mM Hepes, pH 7.5, 150 mM NaCl, 0.5% BSA) for 30 min at 37 °C. Chromogenic substrate (final concentration 200 μM) was then added and the reaction mixture incubated for 90 min at 37 °C. Aliquots were taken, and substrate hydrolysis was estimated by end point reading at 405 nm, using a Thermomax microplate reader. Experiments were performed in quadruplicate.

Determination of in Vitro α-Thrombin Generation. Human platelet-poor plasma (500 μL) was activated by addition of 16 μL of APTT reagent (cephalin plus ellagic acid) and 20 μL of $CaCl_2$ 0.5 M in the presence or absence of anophelin. At 15-s time intervals, 10 μL of activated plasma was removed into 200 μL of substrate solution (200 μM S-2238 in Hepes−BSA, pH 7.4). After 10 min, 50 μL of glacial acetic acid was added, and absorbance was measured at 405 nm against a blank. This assay measures free, uninhibited α-thrombin rather than total α-thrombin production. The amidolytic activity of α-thrombin is expressed as the equivalent amount of α-thrombin considering an activity of 3 mOD/min/nM of α-thrombin.

Estimation of Protein Concentration. Anophelin concentration was estimated by measuring protein absorbance at 280 nm (Perkin-Elmer, UV/VIS spectrometer Lambda 18).

Statistical Analysis. Data were analyzed by Jandel SigmaStat 2.0 statistical software (Jandel Corp.) and are reported as means ± SE.

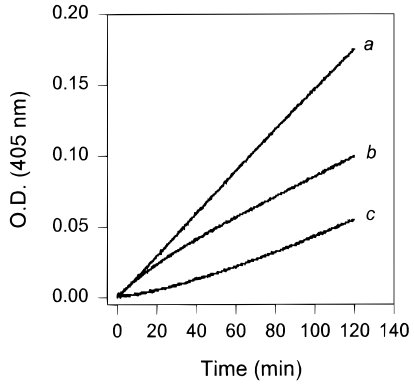

FIGURE 1: Typical progress curves for α-thrombin-mediated S-2238 hydrolysis in the absence (curve a) and presence of anophelin (curves b and c). Curve b: reaction was started by the addition of α-thrombin (50 pM) to a mixture containing anophelin (300 pM) and S-2238 (500 μM). Curve c: reaction was started by the addition of S-2238 (500 μM) after 30-min preincubation of α-thrombin (50 pM) and anophelin (300 pM) at 37 °C. Substrate hydrolysis was followed for 2 h at 37 °C, at 405 nm.

RESULTS AND DISCUSSION

We have previously shown that synthesized anophelin behaves in vitro as a tight α-thrombin inhibitor with an apparent K_i of ~100 pM (*22*). In the present study, we further investigated the mechanism of α-thrombin inhibition by anophelin by both kinetics and biochemical assays.

Preliminary experiments involving preincubation of anophelin with α-thrombin at room temperature for 30 min prior to the addition of substrate showed a product progress curve with an upward concavity (Figure 1, curve c). However, when α-thrombin was added to the reaction medium containing anophelin, the progress curve displayed a downward concavity (Figure 1, curve b). This experiment indicates that the interaction of anophelin with α-thrombin displays slow-binding kinetics as seen with many peptidic inhibitors of serine proteinases (*24*−*27*).

In addition to exhibiting slow-binding kinetics, anophelin significantly inhibits α-thrombin at concentrations similar to that of the enzyme (Figures 1 and 2) (*22*), indicating that anophelin is also a tight-binding inhibitor (*24*−*27*). Conventional Michaelis−Menten kinetics does not apply to the study of tight-binding inhibitors, because it assumes that the free inhibitor concentration is equal to the total inhibitor concentration, a condition met when the enzyme used is at a much lower concentration than the inhibitor. Therefore, Morrison's equation for tight-binding inhibition (*24, 25*) was used to obtain apparent dissociation constants for anophelin:

$$V_s/V_o = \{([E_t] - [I_t] - K_i^*) + ([I_t] + K_i^* - [E_t])^2 + 4K_i^*[E_t]^{1/2}\}/2[E_t] \quad (1)$$

where K_i^* is the apparent dissociation constant for the enzyme−inhibitor complex, V_s is the inhibited steady-state velocity, V_o is the control (uninhibited) velocity, $[I_t]$ is the total inhibitor concentration, and $[E_t]$ is the total α-thrombin concentration. In these experiments, the enzyme (50 pM) was allowed to interact for 1 h with inhibitor (0−600 pM), in the presence of several concentrations of substrate, before product rate formation for the following 30 min was recorded. Resulting steady-state rates were fit by nonlinear regression to eq 1 for several substrate concentrations. Figure 2 shows V_s/V_o plotted against anophelin concentration for a 500 μM substrate concentration, the line being the best sum of squares fit obtained with a K_i^* of 63 pM. When the K_i^* for several substrate concentrations was plotted against the substrate concentration, a linear regression line ($r^2 = 0.9941$) indicated a y intercept of 5.87 ± 1.46 pM (Figure 2, inset), which is an estimate of anophelin's K_i for α-thrombin. This experiment also indicates that the inhibition is competitive and follows the expression:

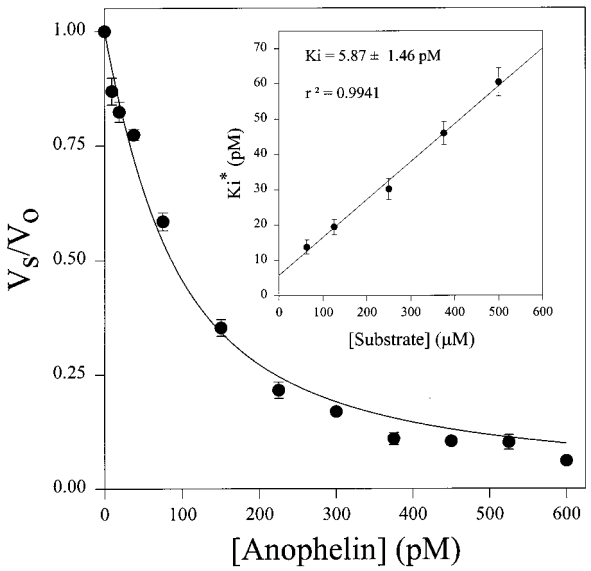

FIGURE 2: Kinetics of the inhibition of α-thrombin-induced chromogenic substrate (S-2238) hydrolysis by anophelin. Determination of the apparent dissociation constant, K_i^*, from steady-state velocities. The reactions were initiated by the addition of α-thrombin (50 pM) to a mixture containing anophelin and S-2238 at 500 μM; reactions were followed for 2 h at 37 °C. The solid line represents the best nonlinear fit of the data to eq 1, yielding a K_i^* of 67 pM. Inset: relationship of the apparent dissociation constant, K_i^*, to substrate concentration, when reactions were initiated by the addition of α-thrombin. Values for K_i^* were calculated as described in the text (α-thrombin, 50 pM; anophelin, 0−600 pM; chromogenic substrate, 37.5−500 μM). Linear regression of the data yields a K_i of 5.87 pM ($r = 0.9941$). The points in each figure are the mean ± SE of six independent experiments.

Scheme 1

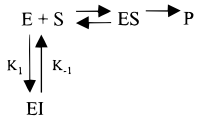

Scheme 2

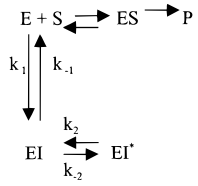

$$K_i^* = K_i(1 + [S]/K_m) \quad (2)$$

Slow-binding, competitive inhibition can be described by at least two mechanisms (*24, 25*). Scheme 1 predicts the formation of a single EI complex, while Scheme 2 postulates the rapid formation of an EI complex which then slowly isomerizes to a more stable complex (EI*). In Scheme 1 there

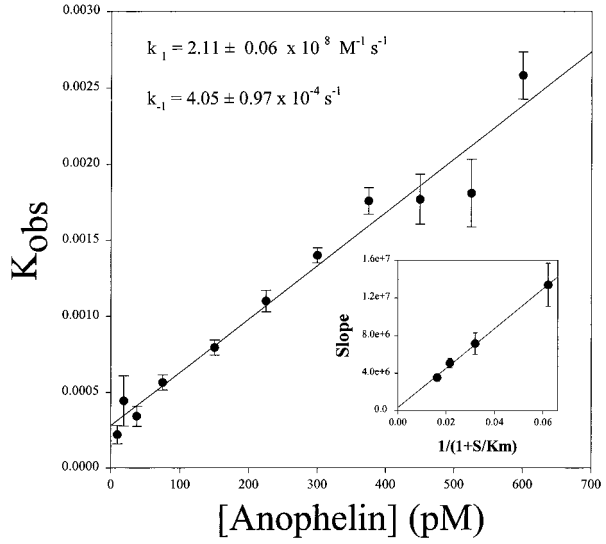

FIGURE 3: Relationship between the apparent first-order rate constant, k_{obs}, and the concentration of anophelin. Progress curves were generated with 500 μM S-2238, 0−600 pM anophelin, and 50 pM α-thrombin. The apparent first-order rate constant was calculated by using nonlinear regression fit of the data to eq 5, yielding $K_1 = 2.11 \pm 0.06 \times 10^8$ M^{-1} s^{-1}, $K_{-1} = (0.554 \pm 0.178) \times 10^{-3}$ s^{-1}, and $K_i^* = 1.91$ pM, where $K_m = 8.3$ μM (summary of six experiments). Inset: plots of the slope ($K_i/(1 + [S]/K_m)$ of the main figure and three additional curves at different substrate concentrations against $1/(1 + [S]/K_m)$. The regression equation produced a $r^2 = 0.998$.

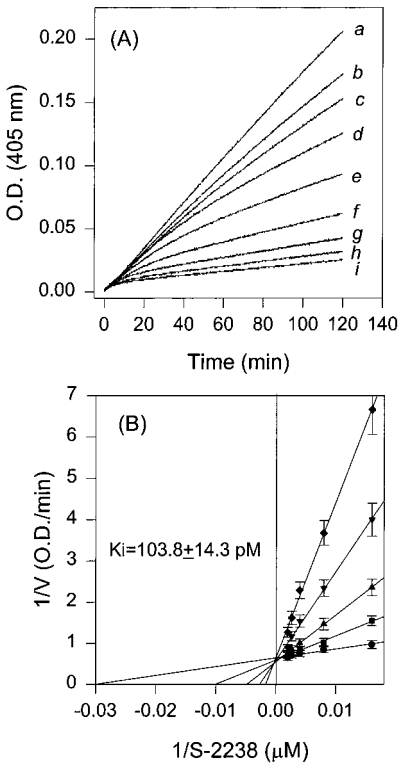

FIGURE 4: Effects of NaCl on the inhibition constant of anophelin−α-thrombin complex. (A) Progress curves were obtained by addition of α-thrombin (50 pM) to a mixture containing anophelin (a, 0 nM; b, 0.625 nM; c, 1.25 nM; d, 2.5 nM; e, 5 nM; f, 10 nM; g, 20 nM; h, 30 nM; i, 40 nM) and chromogenic substrate (S-2238, 250 μM) in the presence of 0.15 M NaCl. A representative experiment is shown ($n = 7$). (B) Double-reciprocal plot of the inhibition of α-thrombin by anophelin (●, 0.625 nM; ■, 1.25 nM; ▲, 2.5 nM; ▼, 5 nM; ◆, 10 nM) at different substrate concentrations (62.5−500 μM). The K_i was obtained by using eq 2, yielding a K_i of 103.8 ± 14.3 pM. The points in each figure are the mean ± SE of seven independent experiments.

is a linear relationship between inhibitor concentration and the apparent first-order rate constant, k_{obs} (eq), while Scheme 2 predicts a hyperbolic relationship (eq 4), where $K_{i,app} = (K_i(1 + [S]K_m)$ and $K_i = k_{-1}/k_1$:

$$k_{obs} = k_{-1} + k_1[I]/(1 + [S]/K_m) \quad (3)$$

$$k_{obs} = k_{-2} + k_2[I]/([I] + K_{i,app}) \quad (4)$$

To obtain k_{obs}, progress curves of product formation by α-thrombin (not preincubated with inhibitor) were analyzed by using the rate equations of Morrison (*24*, *25*) and Cha (*26*):

$$P = V_s t + (V_o - V_s)(1 - e^{-k_{obs}\, t})/k_{obs} \quad (5)$$

The integrated first-order rate equation describes the slow establishment of equilibrium between enzyme and inhibitor where P is the measured absorbance defined as a function of initial (V_o) and final (V_s) steady-state velocities and the apparent first-order rate constant, k_{obs}, which describes the equilibration from the initial to the final steady state (*27*). Progress curves obtained in different inhibitor and substrate concentrations were fit by nonlinear regression to eq 5 to obtain k_{obs} at different inhibitor and substrate concentrations. Plots of k_{obs} thus obtained against anophelin (0−600 pM) concentrations were fit by linear regression, with a correlation coefficient higher than 0.95 for each of the four substrate concentrations used (Figure 3). The plots did not indicate a hyperbolic relationship as proposed by Scheme 2. We conclude that Scheme 1 is a good model for the interaction of anophelin with α-thrombin.

According to eq 3, k_{-1} can be estimated from the y axis intercepts of k_{obs} vs inhibitor plots (Figure 3). The slope of such graphs represents the expression $k_1/(1 + [S]/K_m)$. A plot of these slopes obtained at several substrate concentrations, plotted as a function of $1/(1 + [S]/K_m)$, should thus yield a straight line crossing the origin, with a slope numerically equal to k_1 (Figure 3, inset). We thus obtained a $k_1 = 2.11 \pm 0.06 \times 10^8$ M^{-1} s^{-1} and a k_{-1} of $4.05 \pm 0.97 \times 10^{-4}$ s^{-1} (mean ± SE). Since $K_i = k_{-1}/k_1$, an independent estimate of K_i is obtained (1.91 pM), which is in reasonable agreement (considering the standard errors involved) with the K_i of 5.87 pM obtained previously, with a different set of experiments and equations. These experiments also implicitly confirm the competitive nature of the inhibition of α-thrombin by anophelin.

The kinetic constants obtained above were found in low ionic strength conditions. Because anophelin is a highly charged molecule (*22*), higher ionic strength could increase anophelin's K_i by decreasing ionic interactions between the enzyme and the inhibitor. Accordingly, we next tested the effects of salt concentration on the affinity of anophelin−α-thrombin. At 0.15 M NaCl, anophelin behaves as a typical slow-binding inhibitor (Figure 4A), and considerably higher concentrations of the inhibitor (0.625−40 nM) were necessary for inhibition of α-thrombin (50 pM) (Figure 4A). At such salt concentrations, anophelin concentration is far above enzyme concentration, as described for many classical

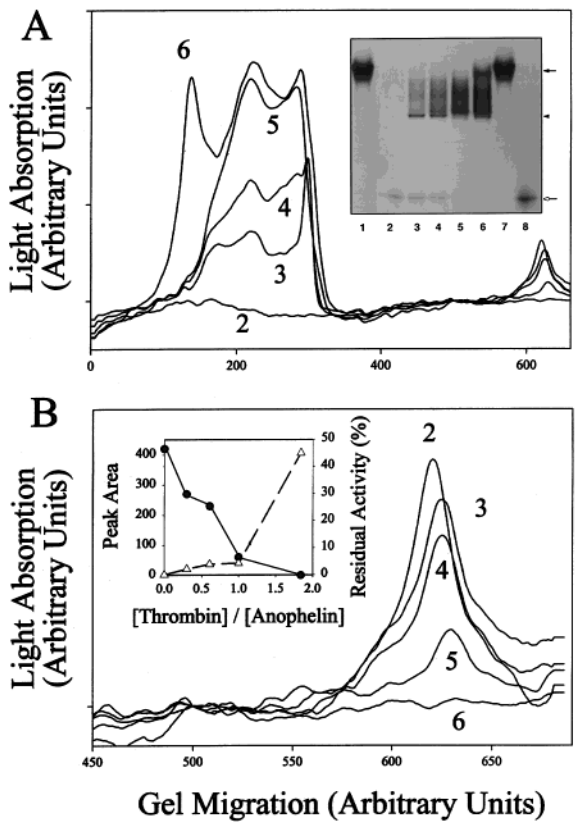

FIGURE 5: Anophelin binds to α-thrombin. (A) Band densitometry and nondenaturing gel electrophoresis (inset) of anophelin−α-thrombin complex. Anophelin (4.5 μM, lanes 3−6) was incubated with increasing concentrations of α-thrombin (lanes 3−6). Lane 3, α-thrombin (1.38 μM); lane 4, α-thrombin (2.76 μM); lane 5, α-thrombin (4.5 μM); lane 6, α-thrombin (8.3 μM); lanes 1 and 7, α-thrombin (8.3 μM); lane 2, anophelin (4.5 μM); lane 8, anophelin (33.2 μM). Inset: arrows, α-thrombin; arrowhead, anophelin−α-thrombin complex; open arrows, anophelin. (B) Band densitometry showing the disappearance of the band corresponding to anophelin (inset, right *y* axis, closed circles) and the appearance of α-thrombin activity (inset, left *y* axis, open triangles) with increasing α-thrombin−anophelin molar ratios. PAGE was performed in 4−20% gels, under nondenaturing conditions. Figure is a representative experiment ($n = 3$).

enzyme inhibitors. Double-reciprocal plots were used to calculate the K_i*, and by using the expression $K_i^* = K_i(1 + [I]/K_m)$, a K_i of 103.8 ± 14.3 pM was obtained (Figure 4B). At 0.4 M NaCl, a K_i of 1.22 nM was calculated (data not shown). The increase in the K_i observed at higher salt concentrations suggests that ionic interactions mediate anophelin−α-thrombin complex formation.

To study the direct interaction of enzyme and inhibitor, increasing concentrations of α-thrombin (1.38−8.3 μM) were added to a fixed concentration of anophelin (4.5 μM). Complex formation and the disappearance of the band corresponding to anophelin were detected by nondenaturing gel electrophoresis (Figure 5A, inset) and quantified by band densitometry (Figure 5A,B). The area corresponding to anophelin was plotted against different enzyme/inhibitor molar ratios (Figure 5B, inset, left *y* axis, closed circles), and the detection of the residual catalytic activity of α-thrombin was performed by means of chromogenic assay (Figure 5B, inset, right *y* axis, open triangles). Figure 5A, and inset, shows that anophelin (4.5 μM) is stained as a fast migrating protein (lane 2), whereas α-thrombin (8.3 μM) behaves as a slow-speed migrating protein, in the absence of inhibitor (lanes 1 and 7). In the presence of 1.26 and 2.76 μM anophelin (Figure 5A, lanes 3 and 4, respectively), α-thrombin migrates as a broad band of faster-speed migrating behavior than the noncomplexed molecule, whereas anophelin (4.5 μM), which is in excess, can be detected as a single band (Figure 5A,B, inset). At this enzyme/inhibitor molar ratio, the catalytic activity of α-thrombin is almost completely blocked (Figure 5B, inset). When 4.5 μM anophelin was incubated with 4.5 μM α-thrombin, a broad band with a fast migration pattern was detected (Figure 5, lane 5), together with an almost complete disappearance of anophelin (Figure 5A,B, insets) and more than 95% inhibition of α-thrombin catalytic activity (Figure 5B, inset). Lane 6 shows that when an excess of α-thrombin is present, yielding an α-thrombin/anophelin molar ratio of 1.84, enzyme's residual activity is ~45%, and anophelin cannot be detected in the gel as a single fast-migrating band; in addition, part of α-thrombin behaves like the noncomplexed molecule. This finding indicates that enzyme−inhibitor formation occurs at a 1:1 molar concentration. Interaction of anophelin is specific for α-thrombin, since incubation of anophelin (10 μM) with prothrombin (6.9 μM), factor X (6.9 μM), or factor Xa (6.9 μM) followed by resolution of complex formation by nondenaturing gel electrophoresis did not modify the migration pattern of the factors tested (data not shown, ref *22*). In addition, incubation of anophelin (6.75 μM) with α-thrombin (8.3 μM) for up to 6 h at 37 °C, followed by separation of the complex with Laemmli buffer, boiling, and 4−20% SDS−PAGE, did not modify the amount of anophelin detected as a low molecular weight protein, suggesting that cleavage of anophelin did not take place (data not shown).

α-Thrombin has two main functional domains: the catalytic site, which cleaves fibrinogen, and TABE1, which mediates α-thrombin interaction with a number of molecules including fibrinogen, protein C, thrombomodulin, and α-thrombin receptor (*5*−*7*, *10*). One additional site, TABE2, has been described; it mediates α-thrombin binding to heparin−antithrombin III complex (*13*, *14*).

In an attempt to identify the role of α-thrombin functional domains on the inhibitory properties of anophelin, a number of experiments were performed using γ-thrombin. γ-Thrombin is produced by limited proteolysis of α-thrombin by trypsin, where TABE1 is disrupted (*1*, *26*, *27*). We then performed kinetics experiments to calculate the affinity of the anophelin−γ-thrombin complex. Anophelin was incubated with chromogenic substrate, followed by addition of γ-thrombin. In contrast to its effects on α-thrombin, anophelin behaves as a fast and classical inhibitor of γ-thrombin (Figure 6A). Inhibition is observed at an anophelin concentration far above the enzyme concentration (Figure 6A), and a K_i of 0.69 ± 0.063 nM was calculated by double-reciprocal plot for competitive, classical enzyme inhibitors (Figure 6B). The larger K_i for anophelin when using γ-thrombin, together with the effects of NaCl in the dissociation constant of anophelin vs α-thrombin interaction, strongly suggests that TABE1 is involved in the interactions of anophelin with α-thrombin. When γ-thrombin (5 μM) is incubated with anophelin (10 μM), followed by nondenaturing electrophoresis of the mixture, a shift of γ-thrombin is achieved (Figure 6C, lanes 1 and 2) that reaches a maximum when the anophelin−γ-thrombin molar ratio is 1 (not shown). These results provide

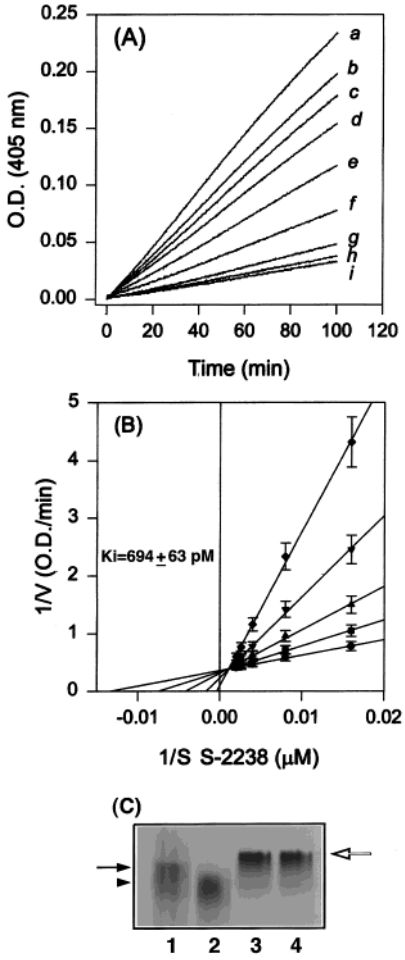

FIGURE 6: Anophelin interaction with γ-thrombin. (A) Progress curves showing the fast-binding inhibition of γ-thrombin by anophelin. Anophelin (a, 0 nM; b, 1.125 nM; c, 2.25 nM; d, 4.5 nM; e, 9 nM; f, 18 nM; g, 36 nM; h, 54 nM; i, 72 nM) was incubated for 15 min with chromogenic substrate (250 μM) followed by the addition of γ-thrombin (0.45 nM). A representative experiment is shown ($n = 4$). (B) Apparent K_i* from steady-state velocities was determined by addition of γ-thrombin (0.45 nM) to a mixture containing various concentrations of anophelin (●, 1.125 nM; ■, 2.25 nM; ▲, 4.5 nM; ▼, 9 nM; ◆, 18 nM) and chromogenic substrate (62.5−500 μM). Double-reciprocal plot of the data yields a K_i of 0.694 ± 0.063 nM. (C) Anophelin binds to γ-thrombin but not to PPACK-γ-thrombin. Complex formation was detected by 4−20% nondenaturing PAGE, and proteins were stained by Coomassie Blue. Lane 1, γ-thrombin (4 μM); lane 2, γ-thrombin (4 μM) and anophelin (10 μM); lane 3, PPACK-γ-thrombin (4 μM); lane 4, PPACK-γ-thrombin (4 μM) and anophelin (10 μM). Arrow, γ-thrombin; arrowhead, anophelin−γ-thrombin complex; open arrow, PPACK-treated γ-thrombin. The figure is a representative experiment ($n = 3$).

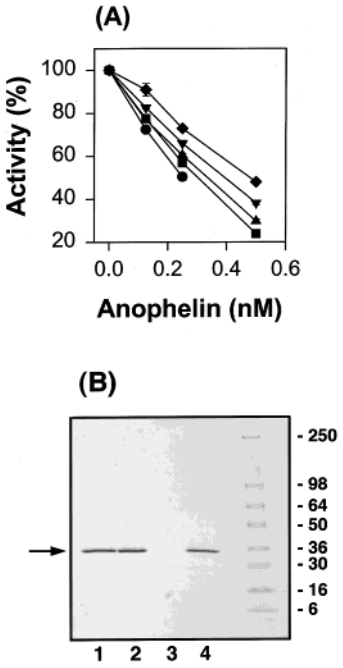

FIGURE 7: Anophelin binds to TABE1. (A) Effects of C-terminal hirudin fragment 54−65 on α-thrombin inhibition by anophelin. Thrombin (0.75 nM) was incubated at 37 °C for 10 min with (●) buffer or (■) 0.5, (▲) 1, (▼) 2, or (◆) 4 μM C-terminal hirudin fragment 54−65, followed by addition of anophelin and 200 μM chromogenic substrate. The points in each figure are the mean ± SE of duplicate experiments ($n = 3$). (B) Inhibition of trypsin-mediated α-thrombin proteolysis by anophelin. α-Thrombin (4.1 μM, 47 pmol) was incubated with buffer (lanes 1 and 3) or anophelin (10 μM; lanes 2 and 4) for 10 min in the absence (lanes 1 and 2) or presence (lanes 3 and 4) of 250 ng of trypsin. Mixtures were incubated for 1 h at 37 °C, and reactions were terminated by addition of Laemmli buffer and boiling for 5 min. Formation of complex was performed by SDS−PAGE; proteins were stained by Coomassie Blue.

direct evidence that anophelin binds to γ-thrombin, most likely by interaction with the catalytic site. Since TABE2 is present in γ-thrombin, it was of interest to determine whether the catalytic site was the sole domain involved in anophelin−γ-thrombin interaction. Thus, γ-thrombin was incubated with PPACK, a reagent that irreversibly modifies the catalytic site of thrombin by alkylating active-site histidine (*28*). Figure 6C shows that PPACK-γ-thrombin (lane 3) has a slower migration pattern than does nontreated γ-thrombin (lane 1). When PPACK-γ-thrombin was incubated with an excess of anophelin, its migration pattern did not change (lane 4), in contrast to nontreated γ-thrombin (lane 2). Similar results have been obtained with PPACK-α-thrombin, whose migration is not modified by anophelin (data not shown). These results imply that the catalytic site is important for interaction of anophelin with α-thrombin, in agreement with the data above indicating competitive kinetics with small chromogenic substrates.

Anophelin is an acidic protein (p*I* 3.52), containing 17 (out of 60) strongly acidic amino acids in its sequence: 10 aspartic acids and 7 glutamic acids. The possible contribution of TABE1 in the interaction of α-thrombin with anophelin was then further studied by means of two complementary protocols. First, increasing C-terminal hirudin fragment 54−65 concentrations decreases the inhibitory property of anophelin on α-thrombin-mediated chromogenic substrate hydrolysis, with a right-shifted inhibitory dose−response curve (Figure 7A). This finding strongly suggests that anophelin binds to TABE1, because the C-terminal of hirudin binds to TABE1 without affecting the catalytic activity of α-thrombin (*3*, *20*, *30*). Second, it is well-known that trypsin cleaves the Arg73−Asn74 bond of α-thrombin, disrupting the enzyme TABE1 (*27*). Thus, it was of interest to test the effects of anophelin on trypsin-mediated proteolysis of α-thrombin by incubating α-thrombin with trypsin in the presence of inhibitor followed by SDS−PAGE. As expected for a high-affinity TABE1 inhibitor, trypsin-mediated hydrolysis of α-thrombin (Figure 7B, lane 3) was completely blocked by anophelin (lane 4). When α-thrombin was

Table 1: Kinetic Pattern of Anophelin−Thrombin Interactions

	K_i (pM)	type of inhibition	fold decrease in K_i[a]
α-thrombin plus			
0 NaCl	5.87 ± 1.46	slow and tight	
0.15 M NaCl	103.8 ± 14.3	slow and classical	17.6
0.4 M NaCl	1220.0 ± 150	slow and classical	207.8
γ-thrombin (0 NaCl)	694.0 ± 63.52	fast and classical	118.2

[a] Comparison with the K_i obtained for α-thrombin−anophelin interaction, in the absence of NaCl.

incubated with buffer (lane 1) or anophelin (lane 2), formation of the enzyme−inhibitor complex was not obtained, indicating that anophelin−α-thrombin complex is not covalent. Control experiments indicate that anophelin (up to 15 μM, highest concentration tested) does not function as a trypsin inhibitor using a chromogenic substrate (*22*). Anophelin interaction with TABE 1 is substantiated by the finding that its affinity for α-thrombin is dramatically reduced in the presence of salts and it behaves as a lower-affinity, fast inhibitor of γ-thrombin, in comparison to the intact α-thrombin molecule. We conclude that anophelin binds to the catalytic site of α-thrombin and this interaction is strengthened when TABE1 is preserved. In this respect, anophelin resembles hirudin that behaves as a bivalent α-thrombin inhibitor. However, inhibitor sequences are not homologous. Hirudin behaves as a slow-binding inhibitor only at 0.2 M or higher salt concentrations (*31*). Table 1 summarizes the findings concerning the kinetic pattern of the interaction between anophelin and α- or γ-thrombin.

Production of α-thrombin in vivo is accompanied by formation of a clot, and a fraction of α-thrombin remains associated with insoluble fibrin. Although the clot behaves mainly as a trap for α-thrombin, it can also act as a reservoir for active α-thrombin. Clot-bound α-thrombin can cleave fibrinogen and activate factors V and VIII and platelets. This can lead to persistent activation of the coagulation cascade at sites of thrombus formation (*32*−*34*). α-Thrombin in this environment is protected from inhibition by heparin−antithrombin III complex, the current mainstay of antithrombotic therapy (*19*). Heparin acts primarily by accelerating the rate at which antithrombin inactivates α-thrombin and factor Xa. Although heparin is very effective in the prevention and treatment of thromboembolic disorders, one of the most serious limitations of heparin is its inability to catalyze the inactivation of clot-bound α-thrombin. Since anophelin is a small molecule with high affinity for α-thrombin, it was of interest to test its effects on clot-bound α-thrombin. Figure 8 shows that clot-bound α-thrombin-induced chromogenic substrate was inhibited by anophelin in a concentration-dependent manner, with an IC_{50} of 45 nM. Our finding indicates that anophelin—in contrast to heparin and like PPACK, hirulog, and hirudin—can inactivate the α-thrombin bound to fibrin (*34*, *35*).

α-Thrombin generation is triggered by a cascade of enzyme activation leading to an explosive production of the enzyme. In addition, α-thrombin amplifies its own generation by a feed-back mechanism: traces of α-thrombin formed during the initial lag phase activate factors V and VIII, leading to a steep increase in thrombin formation (*23*, *36*, *37*). In an attempt to observe the effects of anophelin in the

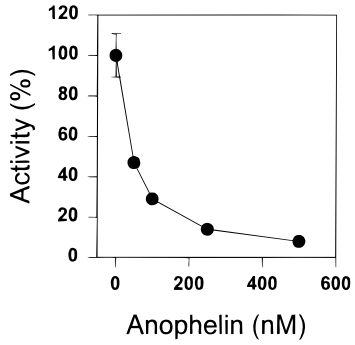

FIGURE 8: Effects of anophelin on clot-bound α-thrombin. Detection of clot-bound α-thrombin was performed as described in Materials and Methods in the presence of increasing concentrations of anophelin, as indicated. Experiments are the mean ± SE of a typical experiment performed in quadruplicate ($n = 3$).

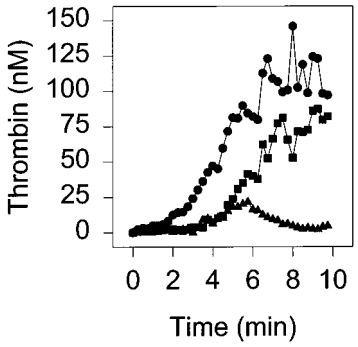

FIGURE 9: Effects of anophelin on α-thrombin generation in plasma. Plasma was incubated with (●) buffer or (■) 0.5 or (▲) 1 μM anophelin. Reactions were initiated by the addition of APTT reagent and $CaCl_2$. Aliquots were removed each 15 s, and thrombin generation was detected by reading of chromogenic substrate hydrolysis at 405 nm as described in Materials and Methods. α-Thrombin concentration was estimated by a titration curve using α-thrombin under the same conditions. The figure represents a typical experiment ($n = 3$).

explosive production of α-thrombin, its production was activated by addition of APTT reagent and $CaCl_2$ to plasma in the presence of increasing concentrations of anophelin; active α-thrombin generation was assessed by measuring chromogenic substrate hydrolysis, using GPRP to prevent fibrinogen polymerization. Figure 9 shows that 500 nM anophelin increases the lag phase of explosive free α-thrombin production. At 1 μM, increase in the lag phase is accompanied by a decrease in the total production of uninhibited α-thrombin. Similar results were obtained with hirudin (data not shown). These findings are consistent with the inhibitory effect of anophelin and hirudin on α-thrombin alone and the absence of effect on other clotting enzymes needed for thrombin formation. Although hirudin has many characteristics for a good antithrombin inhibitor (fast, high affinity, high specificity, noncleavable, only slightly antigenic), one of its limitations in comparison with heparin relates to its moderate inhibitory effect on α-thrombin production (*38*). Actually, many direct α-thrombin inhibitors isolated from blood-sucking insects are likely to have a mild effect on the production of α-thrombin, according to in vitro assays; however, their role as anticoagulant molecules may be relevant in vivo, concerning the feeding necessities of the insect. Accordingly, to achieve efficient blood feeding, most blood-sucking insects have developed more than one

molecule with distinct inhibitory properties and targets, as far as blood coagulation and platelet aggregation are concerned (*39*). We propose that anophelin may work in concert with other antihemostatic components present in the saliva of *A. albimanus*, such as apyrases (*40*), to achieve efficient blood meals. According to its new and unrelated sequence, anophelin may be a useful reagent for studying the structure and function of α-thrombin.

ACKNOWLEDGMENT

The authors thank Brenda Rae Marshall for preparation of this manuscript.

REFERENCES

1. Fenton, J. W., II, Landis, B. H., Walz, D. A., and Finlayson, J. S. (1977) in *Chemistry and Biology of Thrombin* (Lundblad, R. L., Fenton, J. W., and Mann, H. G., Eds.) pp 43−70, Ann Arbor Science Publishers, Ann Arbor, MI.
2. Grutter, M. G., Priestle, J. O., Rahuel, J., Grossenbacher, H., Bode, W., Hofsteenge, J., and Stone, S. R. (1990) *EMBO J. 9*, 2361−2365.
3. Rydel, J. R., Ravichandran, K. G., Tulinsky, A., Bode, W., Huber, R., Roitsch, C., and Fenton, J. W. (1990) *Science 249*, 277−280.
4. Bode, W., Turk, D., and Karshikov, A. (1992) *Protein Sci. 1*, 426−471.
5. Naski, M. C., Fenton, J. W., Maraganore, J. M., Olson, S. T., and Shafer, J. A. (1990) *J. Biol. Chem. 265*, 13484−13489.
6. Tollefesen, D. M. (1995) *Thromb. Haemost. 74*, 1209−1214.
7. Tsiang, M., Lentz, S. R., and Sadler, J. E. (1992) *J. Biol. Chem. 267*, 6164−6170.
8. Wu, Q., Tsiang, M., Lentz, S. R., and Sadler, J. E. (1992) *J. Biol. Chem. 267*, 7083−7088.
9. Jandrot-Perrus, M., Clemetson, K. J., Huisse, M. G., and Guillin, M. C. (1992) *Blood 80*, 2781−2786.
10. Guillin, M. C., Bezeaud, A., Bouton, M. C., and Jandrot-Perrus, M. (1995) *Thromb. Haemost. 74*, 129−133.
11. De Marco, L., Mazzucato, M., Masotti, A., and Ruggeri, Z. M. (1994) *J. Biol. Chem. 269*, 6780−6784.
12. Bouton, M. C., Jandrot-Perrus, M., Moog, S., Cazenave, J. P., Guillin, M. C., and Lanza, F. (1995) *Biochem. J. 305*, 635−641.
13. Stubbs, M. T., and Bode, W. (1993) *Trends Biochem. Sci. 20*, 23−28.
14. Gan, Z. R., Li, Y., Chen, Z., Lewis, S. D., and Shafer, J. A. (1994) *J. Biol. Chem. 269*, 1301−1305.
15. Noeske-Jungblut, C., Haendler, B., Donner, P., Alagon, A., Posaani, L., and Schleuning, W. (1995) *J. Biol. Chem. 270*, 28629−28634
16. Markwardt, F., and Walsmann, P. (1967) *Hoppe-Seyler's Z. Physiol. Chem. 348*, 1381−1386.
17. Arocas, V., Zingali, R. B., Guillin, M. C., and Bon, C. (1996) *Biochemistry 35*, 9083−9089.
18. Francischetti, I. M. B., Monteiro, R. Q., and Guimarães, J. A. (1997) *Biochem. Biophys. Res. Commun. 235*, 259−263.
19. Stone, S. R., and Tapparelli, C. (1995) *J. Enzyme Inhib. 9*, 3−15.
20. Fareed, J., Callas, D., Hoppensteadt, D. A., Lewis, B. E., Bick, R. L., and Walenga, J. M. (1999) *Sem. Hematol. 36*, 42−56.
21. Jandrot-Perrus, M., Bouton, M. C., Lanza, F., and Guillin, M. C. (1996) *Semin. Thromb. Hemost. 22*, 151−156.
22. Valenzuela, J. G., Francischetti, I. M. B., and Ribeiro, J. M. C. (1999) *Biochemistry 38*, 11209−11215.
23. Ribeiro, J. M. C., Schneider, M., and Guimarães, J. A. (1995) *Biochem. J. 308*, 243−249.
24. Morrison, J. F. (1969) *Biochim. Biophys. Acta 185*, 269−286.
25. Williams, J. W., and Morrison, J. F. (1979) *Methods Enzymol. 63*, 437−463.
26. Cha, S. (1975) *Biochem. Pharmacol. 24*, 2177−2185.
27. Jordan, S. P., Waxman, L., Smith, D. E., and Vlasuk, G. P. (1990) *Biochemistry 29*, 11095−11100.
28. Bode, W., Mayr, I., Baumann, U., Huber, R., Stone, S. R., and Hofsteenge, J. (1989) *EMBO J. 11*, 3467−3475.
29. Dennis, S., Wallace, A., Hofsteenge, J., and Stone, S. R. (1990) *Eur. J. Biochem. 188*, 61−66.
30. Maraganore, J. M., Bourdon, P., Jablonski, J., Ramachandran, K. L., and Fenton, J. W., II (1990) *Biochemistry 29*, 7095−7101.
31. Stone, S. R., and Hofsteenge, J. (1986) *Biochemistry 25*, 4622−4628.
32. Francis, C. W., Markham, R. E., Barlow, G. W., Florback, T. M., Dobrzynski, D. M., and Marder, V. J. (1983) *J. Lab. Clin. Med. 102*, 220−230.
33. Bar Shavit, R., Eldor, A., and Vlodavsky, I. (1989) *J. Clin. Invest. 84*, 1096−1104.
34. Weitz, J., and Hirsh, J. (1993) *J. Lab. Clin. Med. 122*, 364−373.
35. Weitz, J. I., Hudoba, M., Massel, D., Maraganore, J., and Hirsh, J. (1990) *J. Clin. Invest. 86*, 385−391.
36. Ofosu, F. A., Liu, L., and Freedman, J. (1996) *Sem. Thromb. Hemost. 22*, 303−308.
37. Prasa, D., Svendsen, L., and Sturzebecher, J. (1997) *Thromb. Haemost. 77*, 498−503.
38. Stone, S. R., and Maraganore, J. M. (1993) *Methods Enzymol. 223*, 312−336.
39. Ribeiro, J. M. C. (1990) *Infect. Agents Dis. 4*, 143−152.
40. Valenzuela, J. G., Charlab, R., Galperin, M. Y., and Ribeiro, J. M. C. (1998) *J. Biol. Chem. 273*, 30583−30590.

BI991231P